Journal of Materials Chemistry A

Accepted Manuscript

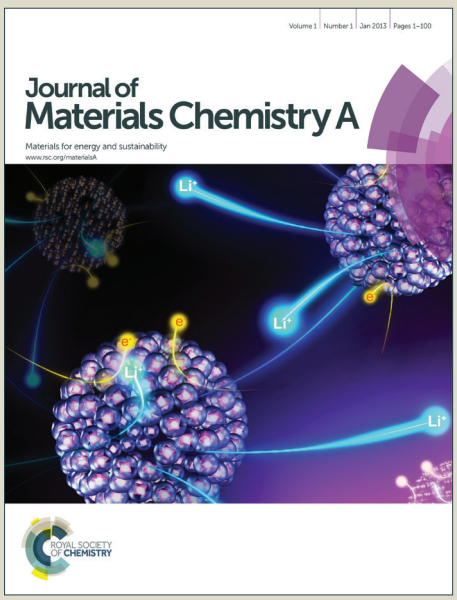

ROYAL SOCIETY OF CHEMISTRY

www.rsc.org/materialsA

Journal Name

RSCPublishing

COMMUNICATION

Honeycomb-Like Single-Wall Carbon Nanotube Networks

Cite this: DOI: 10.1039/x0xx00000x

Shisheng Li, Peng-Xiang Hou, Chang Liu*, Tianyuan Liu, Wen-Shan Li, Jin-Cheng Li and Hui-Ming Cheng

Received 00th January 2012,
Accepted 00th January 2012

DOI: 10.1039/x0xx00000x

www.rsc.org/

A honeycomb-like single wall carbon nanotube (SWCNT) network was constructed by using a paraffin-mediated transfer printing method. Different from random SWCNT nework of similar nanotube density, the honeycomb-like network shows much higher conductivity, transparency and electrical response ability to chemical dopings.

Single-wall carbon nanotubes (SWCNTs) have attracted intense research interest due to their unique electrical, optical, and mechanical properties, and their potential applications in flexible transparent conducting films (TCFs).[1-3] To obtain SWCNT TCFs with a small surface resistance and high optical transparency, great efforts have been devoted to controlling the SWCNT intrinsic properties, such as electronic transport type, crystallinity, length, and bundle size, while their geometrical arrangement, in other word, network morphology is seldom considered.[4, 5] Although various techniques including spin coating, vacuum filtration and inkjet printing have been developed,[6-8] the as-fabricated SWCNT TCFs usually have the similar random network containing entangled SWCNTs and cross-junctions. Both theoretical and experimental studies have proved that the cross-junctions are the major contributors to the resistance of SWCNT thin films.[9, 10] As a consequence, it is highly desirable to eliminate the cross-junctions and provide alternative high conductive channels for carrier transport in the SWCNT networks by optimizing their geometrical arrangement.

Based on mathematical hypothesis, a honeycomb network can cover the maximum area with a minimum number of nodes and shorter line length.[11] This hypothesis is vividly demonstrated in nature and our daily lives. For example, honeybees construct honeycombs with a hexagonal structure; telecom operators build hexagonally distributed cell sites over land areas. These successful applications of honeycomb and other mesh networks have inspired us to explore SWCNT films of honeycomb-like networks. The honeycomb-like networks would dramatically reduce the amount of SWCNTs needed to cover a surface because the total line length is the shortest. The short line length and mesh structure may improve the electrical conductivity. Meanwhile, honeycomb-like networks will expose more surface area without SWCNT coverage, which improves film transparency.

Here, we intentionally use parallel SWCNT arrays as starting SWCNT networks and paraffin as a transfer medium. An ultrathin honeycomb-like network was self-assembled after the transfer printing process. The honeycomb-like networks, mainly composed of SWCNT bundles, show a reduced surface coverage and improved electrical conductivity when compared with random SWCNTs of the similar tube-density. After chemical doping, the honeycomb-like SWCNT network showed a significantly higher increment in conductivity than random SWCNT network.

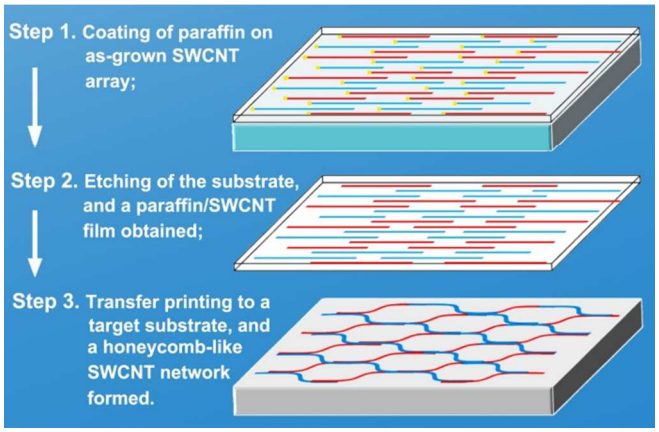

Fig. 1 Schematic showing the paraffin-mediated SWCNT transfer printing process. Step 1, melting and re-solidification of paraffin on the source substrate. Step 2, chemical etching of the source substrate and harvesting of the paraffin/SWCNT film. Step 3, transfer printing of the paraffin/SWCNT film onto a target substrate. After the removal of paraffin by toluene washing, honeycomb-like SWCNT network is obtained.

Fig. 1 schematically shows the paraffin-mediated transfer printing process of a parallel SWCNT array for preparing a honeycomb-like network. The array was grown on the surface of a ST-cut quartz substrate by the chemical vapor deposition of ethanol at 900 ^{o}C. The quartz substrate with the grown parallel SWCNT array was then covered by liquid paraffin by placing a piece of the solid paraffin on its surface and melting it at ~60

°C. Due to the high wettability of the liquid paraffin, the SWCNTs were embedded in the paraffin film when it re-solidified at room temperature (~25 °C). Next, the quartz substrate was etched away by immersing it in hydrofluoric acid, and a paraffin/SWCNT film lifted off and floated to the surface of the acid. The paraffin/SWCNT film is self-standing and rigid enough to be handled and transferred to target Si/SiO_2 substrates. For clarity, optical images of transfer steps 1 and 2 are shown in Fig. S1 (ESI). Finally, the paraffin was removed by immersing the sample in toluene for several times. After the evaporation of residual toluene, a honeycomb-like SWCNT network was self-assembled.

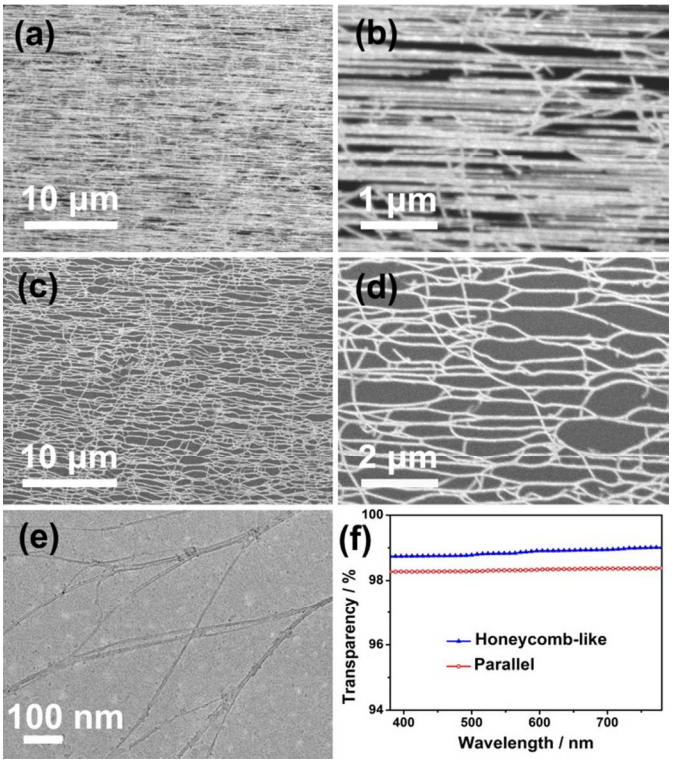

Fig. 2. (a) SEM image of the as-grown parallel SWCNT array on a ST-cut quartz substrate. (b) Enlarged view showing the high-density of the parallel SWCNT array and that only a few SWCNTs are misaligned. (c) A Honeycomb-like network formed after transferring onto a target Si/SiO_2 substrate using paraffin as a mediator. (d) Enlarged view of the honeycomb-like SWCNT network. (e) Typical TEM image of the transferred honeycomb-like SWCNT network. (f) Optical transmittance spectra of two kinds of SWCNT networks: parallel and honeycomb-like SWCNTs.

As can be seen in Figure 2a, the as-grown SWCNTs on the quartz substrate form an array of parallel individual SWCNTs. The SWCNT array has a high coverage of the substrate surface, which can be further verified from a magnified SEM view (Fig. 2b) that shows a density of ~6 tubes/μm. After transfer printing, a honeycomb-like SWCNT network was formed as shown in Fig. 2c and 2d, and the network consists of mainly SWCNT bundles with a density of ~2 bundles/μm. We attribute the formation of the honeycomb-like network to the following reasons. First, the capillary force ($F_{capillary}$) generated by the evaporation of toluene. Second, the moderate interaction between SWCNTs and the Si/SiO_2 substrate ($F_{interaction}$). When $F_{capillary} > F_{interaction}$, capillary force can draw adjacent tubes to form a bundle, like a zipper. (Fig. S2, ESI). Due to the fact that the coverage of a bundle is much smaller than the sum of all its individual SWCNTs, the surface coverage in the honeycomb-like network greatly decreases as shown in Fig. S3 and Table S1 (ESI). The larger exposure area of the honeycomb-like SWCNT networks will improve the transparency when used as TCFs. Thanks to the randomly distributed catalyst nanoparticles, the as-grown parallel SWCNTs have different nucleation sites. Thus, it is possible that one SWCNT bridges two small bundles (Fig. 1 and Fig. S2, ESI). This is vitally important to form a multi-channel conductive network and dramatically increase the contact area between adjacent SWCNTs in the honeycomb-like networks. From the TEM image of Fig. 2e, we can see that the SWCNTs have a clean surface after transfer printing. Small SWCNT bundles are inter-connected and some even form large bundles, which provide a "highway" for carrier transport.

Optical transparency and electrical conductivity are the two most important properties of SWCNT TCFs.[1-3, 12] However, it is difficult to achieve high electrical conductivity without sacrificing optical transparency. Here, We used monolayer honeycomb-like and random SWCNT networks for comparison. We observed a simultaneous increase of optical transparency and electrical conductivity of the honeycomb-like SWCNT network when compared with random SWCNT network. Fig. 2f shows the optical transmittance spectra of two kinds of SWCNT networks: parallel and honeycomb-like SWCNTs. Optical transmittance measurements showed that the as-grown SWCNT array (~6 tubes/μm) has an optical transparence of ~98.4% at 550nm. After paraffin-mediated transfer printing, the honeycomb-like SWCNT network showed an improved transparency of ~98.9%, which can be attributed to the increased exposed area by forming SWCNT bundles as shown in Fig. 2 and Fig. S3 (ESI).

In the left column of Fig. 3, we show I-V curves of a parallel SWCNT array, a random SWCNT network with even higher tube density (~8 tubes/μm), and a honeycomb-like network obtained by paraffin-mediated transfer. For the parallel SWCNT array of 4 mm long and 5 mm wide, the channel resistance is 284 kΩ. While the channel resistance of the corresponding honeycomb-like SWCNT network is only 7.1 kΩ, showing that the channel conductivity improved by a factor of ~40 after the transfer printing. We attributed the great improvement in channel conductivity to the formation of interconnected SWCNT bundles in the honeycomb-like network, instead of isolated SWCNTs in the initial parallel SWCNT array, which provides multi-channels for carrier transport and greatly improve the carrier hopping probability. It is interesting to note that even though the random SWCNT network has a higher nanotube density, its channel resistance (9.8 kΩ) is higher than that of the honeycomb-like SWCNT network, which is abnormal to the knowledge we gain from previous study on SWCNT TCFs, i.e., thicker SWCNT films usually have higher electrical conductivity.[2] These results can be ascribed to the distinct differences in network morphologies. In random networks, the contact area of cross-junctions is very limited due to the small diameter of SWCNTs. Yang, *et al.* reported that the contact geometry has a strong influence on the conductivity of SWCNT cross-junctions. They demonstrated three junction geometries labeled HH (hollow-hollow), HC (hollow-carbon) and CC (carbon-carbon), depending on how one nanotube is aligned relative to the other. Density functional theory calculations showed that the HC and CC geometries have a much smaller conductance than the HH geometries.[13] Due to the limited contact area of SWCNT cross-junctions, it is very difficult to form highly conductive HH geometries which hence reduces the chance of electron hopping between two crossing SWCNTs. In sharp contrast,

due to the helical structure of SWCNTs and large contact area, two intimately-contacted, parallel SWCNTs have more chances to form low-resistance HH geometries along the tubes. Therefore, SWCNT bundles in honeycomb-like networks can effectively increase the electron hopping by forming low resistance HH junctions.

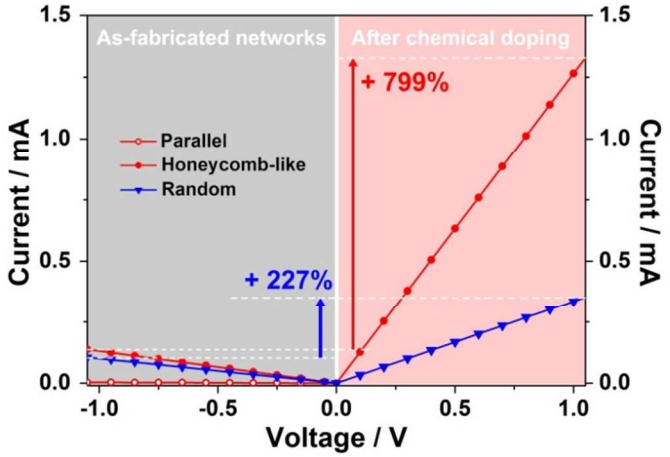

Fig. 3. Left column: I-V curves of the as-grown parallel and random SWCNTs, and as-fabricated honeycomb-like SWCNT network. Right column: I-V curves of the random and honeycomb-like SWCNT networks after HNO_3 doping.

Chemical doping is a commonly used method to improve the conductivity of SWCNT TCFs without sacrificing their transparency. SWCNT TCFs can be doped with HNO_3 solutions, and their surface conductivity is increased by 60-400%.[2, 3, 12, 14-17] In this work, we doped both the random and honeycomb-like SWCNT networks by exposing them to 8 M HNO_3 vapor for 30 min. In the right column of Fig. 3, we show I-V curves of the honeycomb-like and random SWCNT networks after HNO_3 vapor doping. It can be seen that the channel resistance of the random SWCNT network decreased to 3.0 kΩ, corresponding to a conductivity increase by ~230%. Due to the nanometer-size contact area of SWCNT cross-junctions, the resistance decrease is limited. Interestingly, a dramatic decrease of channel resistance was achieved for the honeycomb-like SWCNT network, from the initial 7.1 kΩ to 0.79 kΩ. The conductivity of the honeycomb-like SWCNT network improved by ~800%, the highest increment for doped SWCNT networks ever reported. In this case, chemical doping not only increase the conductivity of SWCNTs, but also reduce the contact resistance of neighboring SWCNTs in bundles. The above results show that the geometrical arrangement of SWCNTs in networks has great effects on their optical transparency, electrical conductivity and their electrical response to chemical doping. The honeycomb-like SWCNT network with high electrical conductivity and high sensitivity to chemical doping shows great promise for use in high-performance TCFs and highly sensitive chemical sensors.

In summary, a honeycomb-like SWCNT network was fabricated by paraffin-mediated transfer printing of a parallel SWCNT array. Compared to the random SWCNT network with similar tube-density, the honeycomb-like SWCNT network shows much higher electrical conductivity. When doped with HNO_3 vapour, the conductivity of the honeycomb-like SWCNT network increased by ~800%. We attributed the high conductivity and high sensitivity to chemical doping of the honeycomb-like SWCNT network to its unique geometry and bundle structure. SWCNT films with such honeycomb-like network structure would be promising for use in high performance TCFs and sensors.

This work was supported by the Ministry of Science and Technology of China (Grants 2011CB932601, 2011CB932604) and National Natural Science Foundation of China (Grants 51221264, 51102242, 51272257).

Notes and references

Shenyang National Laboratory for Materials Science, Institute of Metal Research, Chinese Academy of Sciences, Shenyang 110016, P.R. China
E-mail: cliu@imr.ac.cn
Electronic Supplementary Information (ESI) available: See DOI: 10.1039/b000000x/

1 Z. C. Wu, Z. H. Chen, X. Du, J. M. Logan, J. Sippel, M. Nikolou, K. Kamaras, J. R. Reynolds, D. B. Tanner, A. F. Hebard and A. G. Rinzler, *Science*, 2004, **305**, 1273.
2 W. B. Liu, S. F. Pei, J. H. Du, B. L. Liu, L. B. Gao, Y. Su, C. Liu and H. M. Cheng, *Adv. Funct. Mater.*, 2011, **21**, 2330.
3 A. Kaskela, A. G. Nasibulin, M. Y. Timmermans, B. Aitchison, A. Papadimitratos, Y. Tian, Z. Zhu, H. Jiang, D. P. Brown, A. Zakhidov and E. I. Kauppinen, *Nano Lett.*, 2010, **10**, 4349.
4 R. K. Jackson, A. Munro, K. Nebesny, N. Armstrong and S. Graham, *ACS Nano*, 2010, **4**, 1377.
5 P. E. Lyons, S. De, F. Blighe, V. Nicolosi, L. F. C. Pereira, M. S. Ferreira and J. N. Coleman, *J. Appl. Phys.*, 2008, **104**, 044302.
6 J. W. Jo, J. W. Jung, J. U. Lee and W. H. Jo, *ACS Nano*, 2010, **4**, 5382.
7 M. A. Meitl, Y. X. Zhou, A. Gaur, S. Jeon, M. L. Usrey, M. S. Strano and J. A. Rogers, *Nano Lett.*, 2004, **4**, 1643.
8 W. R. Small and M. I. H. Panhuis, *Small*, 2007, **3**, 1500.
9 M. P. Garrett, I. N. Ivanov, R. A. Gerhardt, A. A. Puretzky and D. B. Geohegan, *Appl. Phys. Lett.*, 2010, **97**, 163105.
10 P. N. Nirmalraj, P. E. Lyons, S. De, J. N. Coleman and J. J. Boland, *Nano Lett.*, 2009, **9**, 3890.
11 R. Kershner, *Am. J. Math.*, 1939, **61**, 665.
12 H. Z. Geng, K. K. Kim, C. Song, N. T. Xuyen, S. M. Kim, K. A. Park, D. S. Lee, K. H. An, Y. S. Lee, Y. Chang, Y. J. Lee, J. Y. Choi, A. Benayad and Y. H. Lee, *J. Mater. Chem.*, 2008, **18**, 1261.
13 F. A. Bulat, L. Couchman and W. T. Yang, *Nano Lett.*, 2009, **9**, 1759.
14 A. A. Green and M. C. Hersam, *Nat. Nanotechnol.*, 2009, **4**, 64.
15 R. Jackson, B. Domercq, R. Jain, B. Kippelen and S. Graham, *Adv. Funct. Mater.*, 2008, **18**, 2548.
16 K. K. Kim, S. M. Yoon, H. K. Park, H. J. Shin, S. M. Kim, J. J. Bae, Y. Cui, J. M. Kim, J. Y. Choi and Y. H. Lee, *New J. Chem.*, 2010, **34**, 2183.
17 H. Tantang, J. Y. Ong, C. L. Loh, X. C. Dong, P. Chen, Y. Chen, X. Hu, L. P. Tan and L. J. Li, *Carbon*, 2009, **47**, 1867.